RESEARCH ARTICLE

Global sensitivity analysis of certain and uncertain factors for a circular tunnel under seismic action

Nazim Abdul NARIMAN[a*], **Raja Rizwan HUSSAIN**[b], **Ilham Ibrahim MOHAMMAD**[a], **Peyman KARAMPOUR**[c]

[a] *Department of Civil Engineering, Tishk International University Sulaimani, Sulaimaniya 46001, Iraq*

[b] *Civil Engineering Department, College of Engineering, King Saud University, Riyadh 11421, Saudi Arabia*

[c] *Department of Mechanical Engineering, Faculty of Engineering, Arak University, Arak 38156-875, Iran*

[*] *Corresponding author. E-mail: nazim.abdul@ishik.edu.iq*

ABSTRACT There are many certain and uncertain design factors which have unrevealed rational effects on the generation of tensile damage and the stability of the circular tunnels during seismic actions. In this research paper, we have dedicated three certain and four uncertain design factors to quantify their rational effects using numerical simulations and the Sobol's sensitivity indices. Main effects and interaction effects between the design factors have been determined supporting on variance-based global sensitivity analysis. The results detected that the concrete modulus of elasticity for the tunnel lining has the greatest effect on the tensile damage generation in the tunnel lining during the seismic action. In the other direction, the interactions between the concrete density and both of concrete modulus of elasticity and tunnel diameter have appreciable effects on the tensile damage. Furthermore, the tunnel diameter has the deciding effect on the stability of the tunnel structure. While the interaction between the tunnel diameter and concrete density has appreciable effect on the stability process. It is worthy to mention that Sobol's sensitivity indices manifested strong efficiency in detecting the roles of each design factor in cooperation with the numerical simulations explaining the responses of the circular tunnel during seismic actions.

KEYWORDS shear waves, Sobol's sensitivity indices, maximum principal stress, maximum overall displacement, tensile damage

1 Introduction

The underground structures such as circular tunnels respond to dynamic loads imposed by seismic actions in different way compared to that of above ground structures, where these tunnels do not undergo resonance with the surrounding ground but their responses are dependent on the response of the surrounding ground. The effect of seismic loads on tunnels is described through the imposed deformations from the surrounding media. The design of tunnels is conducted to accommodate these deformations. The loads imposed by the earthquakes are generating shear waves vertically which are predominant and cause ovaling deformations in circular tunnels and as a result the distortion of the tunnel lining cross section [1,2].

Many researchers have studied the effect of earthquakes

in circular tunnels and tried to obtain data about the behavior and responses of the structural system using finite element analysis in addition to stochastic methods. Nariman et al. [3] have performed numerical analysis and simulation of a circular tunnel with uncertain three factors related to the surrounding soil during earthquakes. They quantified the uncertainty of those factors which are related to the responses of the tunnel therough meta-models using an experimental method. Nariman et al. [4] studied the structural optimization of four certain factors related to the tunnel lining properties subjected to a ground motion through using coupled XFEM-BCQO approach to analyze the predicted damage in the tunnel lining wher they obtained the optimized values of the factors and predicted the strat of cracks and spalling through using XFEM technique.

Mollon et al. [5] studied the 3D analysis and face stability of a shallow circular tunnel and proposed a

reliability approach adopting the failure modes due to blow-out and the collapse of the ultimate limit state. They discovered that collapse mode of failure result in the most critical deterministic sequences against face stability where they used it in the stochastic analysis and design. They dedicated soil shear strength factors as random variables and quantified the reliability index of Hasofer-Lind in addition to the failure probability. Furthermore, they carried on sensitivity analysis on the soil shear strength factors and finally they performed a reliability-based design to determine the desired tunnel pressure aiming the probability of a target collapse failure.

Kalab and Stemon [6] studied the influence of earthquakes on shallow circular tunnels using three types of rock ground (soft rock, medium hard rock, and hard rock). They performed sensitivity analysis considering Wang's methodology which is soil interaction approach. They variated and tested both the tunnel lining diameter and the Young's modulus of elasticity of the lining, where the thrust force was calculated conditioning no-slip case. They revealed the relations between these factors in the process of the influence of the earthquake on the shallow circular tunnels.

The possible failure of tunnels due to seismic actions might result in damages or in the loss of human lifes. The evaluation of seismic safety for tunnels still a critical problem in the design of tunnel structures which led in development of effective techniques for damage and crack detection [7–17]. To assess the reliability and structural safety of tunnels, advanced computational methods are commonly applied which are capable of capturing the damages. These methods can be classified into continuous and discrete fracture approaches. Continuous approaches to fracture smear the crack over a certain width. They include non-local damage models [18,19] and gradient models [20,21]. Also the introduction of a viscosity [22–26] smears the crack over a certain width. With the seminal work of Miehe et al. [27], phase field approaches have become another alternative to non-local and gradient models. Instead of relating the non-local damage to internal state variables, the damage is obtained by solving a partial differential equations. Phase field approaches have meanwhile been applied to numerous interesting problems [28–34] including fracture in thin shells [33]. Discrete crack approaches include meshfree methods [35–40], extended finite element methods [41–43], smoothed extended finite element methods [44–46], phantom node methods [47–50], extended meshfree methods [51–61], extended IGA [62–65], cracking particle methods [66–73], the numerical manifold method [74–80], efficient remeshing techniques [81–87], multiscale models for fracture [88–100], peridynamics [101–103] and dual-horizon peridynamics [104,105]. One challenge in these methods is tracking the crack path which can become an overworking task especially in 3D and for dynamic fracture.

In this paper we are exploiting Sobol's sensitivity indices which is a variance-based global sensitivity analysis method to quantify the rational effects of seven certain and uncertain factors in the design of circular tunnels related to the damage and stability during seismic actions. This study will reveal the importancy of each factor so that to account for each of which in the design of circular tunnels in conjunction with the numerical simulations using finite element analysis.

2 Finite element model

The 2D model of both the tunnel lining and the soil media generated in ABAQUS program with dimensions details (see Fig. 1) is created to simulate the seismic action for 10 s duration both in vertical and horizontal directions. The tunnel lining thickness, tunnel diameter, tunnel concrete modulus of elasticity, tunnel lining concrete density, peak ground acceleration, soil density, and soil modulus of elasticity are the selected seven certain and uncertain factors respectively to predict the responses of the tunnel regarding the damage in the tunnel lining. The dimensions of the soil media are 50 m $\times$ 100 m. The tunnel lining material is made of reinforced concrete where the reinforcement effect is neglected for simplicity. Concrete damaged plasticity model used for damage detection analysis supporting on real data in the literature, where the dilation angle is 35° and the eccentricity, f_{b0}/f_{c0}, K, and viscosity parameter equal zero for all . Mohr Coulomb plasticity model was used for the soil media to define its shear strengths at different effective stresses (see Table 1). In the initial step two predefined fields were created for the soil, geostatic stress of 20601 Pa and void ratio of 1. A geostatic step of 1 s duration was generated, where the gravity loads of the model system were assigned. Two different boundary conditions were assigned for both the base and the sides of the soil media, by preventing the displacement in x-axis direction for both of them and providing two degrees of freedom for the sides in y-direction and rotation about z-axis for both of them. A static step with duration of 1e−10 s was created for the model system. A dynamic implicit step with 10 s duration was created to simulate the ground motion due to the earthquake by assigning acceleration boundary conditions in both x and y directions with magnitude of 4.905 m/s² . A tie constraint was assigned to model the surface contact between the soil media and the tunnel lining. The soil media and the tunnel lining were modeled with standard plain strain linear with reduced integration hourglass control elements CPE4R.

The model of the circular tunnel has been prepared after performing mesh convergence analysis to obtain the most efficient model which does not changes in the outputs values when further mesh refinements are performed both for the soil and the tunne (Fig. 2). The criteria for the output is the displacement of the a point at the top point
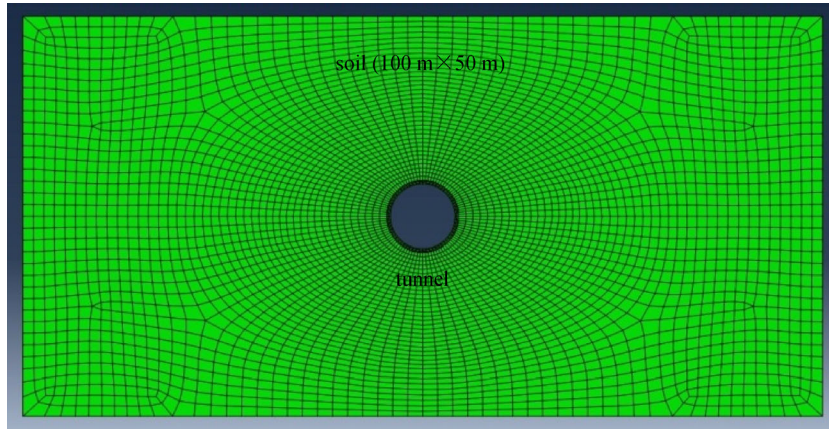
Fig. 1 Finite element model of the circular tunnel

Table 1 Soil Mohr Coulomb plasticity data

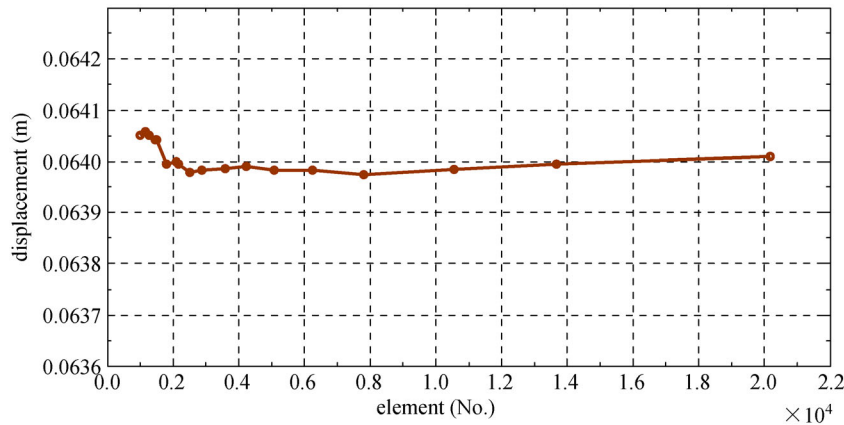| item	friction angle	dilation angle	cohesion yield stress (Pa)	absolute plastic strain
soil plasticity	35°	0°	—	—
soil cohesion	—	—	200000	0

Fig. 2 Mesh convergence analysis

inside the tunnel due to earthquake excitation for the duration of 10 s. Uniform mesh convergence was adopted for the assembly by considering 18 seeding cases starting from 1008 to 20112 total elements. The selected total elements case was 20112 elements where the results of the displacements are constant approximately.

3　Sobol's sensitivity indices

Sobol sensitivity analysis is intended to find out how much of the variability in model output is dependent upon each of the input factors, either upon a single factor or upon an interaction between different factors. The decomposition of the output variance in a Sobol sensitivity analysis employs the same principal as the classical analysis of variance in a factorial design. Sobol sensitivity analysis is not intended to identify the cause of the input variability. It only indicates what impact and to what extent it will have on model output. As a result, it cannot be used to identify the source(s) of variance. The Sobol sensitivity indices is dedicated for seven certain and uncertain factors related to the soil type, tunnel lining properties and the peak ground acceleration.The Sobol's sensitivity indices are ratios of partial variances to total variance, and for independent factors satisfy the relationship:

$$1 = \sum_i s_i + \sum_i \sum_{j>1} s_{ij} + \sum_i \sum_{j>1} \sum_{k>1} s_{ijk} + \cdots. \quad (1)$$

The Sobol' sensitivity indices are:
First effect sensitivity index

$$s_i = \frac{V_i}{V}. \quad (2)$$

Second effect sensitivity index

$$s_{ij} = \frac{V_{ij}}{V}. \quad (3)$$

Total sensitivity index

$$s_{Ti} = s_i + \sum_{j \neq 1} s_{ij} + \cdots. \quad (4)$$

The first effect index, s_i, is a measure for the variance contribution of the individual factor X_i to the total model variance. The partial variance V_i in Eq. (2) is given by the variance of the conditional expectation $V_i = V[E(Y/X_i)]$ and is also called the main effect of X_i on Y. The impact on the model output variance of the interaction between factors X_i and X_j is given by s_{ij} and s_{Ti} is the result of the main effect of X_i and all its interactions with the other factors (up to the pth effect) [106–108].

3.1 Ranges of factors

The certain and uncertain factors under study to quantify the Sobol's sensitivity indices for the damage detection and stability of the circular tunnel under the seismic action are illustrated in the following (Tables 2 and 3) where the name and symbol of each factor would be used in the global sensitivity analysis process.

Table 2 Ranges of certain factors

certain factor	symbol	minimum value	maximum value
tunnel lining thickness (m)	X_1	0.3	0.5
tunnel diameter (m)	X_2	8	10
tunnel lining (concrete) modulus of elasticity (GPa)	X_3	17	31
tunnel lining concrete density (kg/m³)	X_4	2300	2500

Table 3 Ranges of uncertain factors

uncertain factors	symbol	minimum value	maximum value
peak ground acceleration (m/s²)	X_5	0.981	4.905
soil density (kg/m³)	X_6	1800	2200
soil modulus of elasticity (GPa)	X_7	0.2	0.25

4 Results of sensitivity indices — certain factors

The main effects of the sensitivity indices for each certain factor in addition to their interaction effects were calculated targeting the maximum principal stress output of the tunnel lining. Also, the main and interaction effects of sensitivity indices for each certain factor were calculated considering the maximum overall displacement output of the tunnel structure, (see Table 4). Where the main effects of the uncertain factors have been calculated using variation approach, (see Figs. 3 and 4).

Table 4 Sensitivity indices — certain factors

sensitivity indices	maximum principal stress	maximum overall displacement
first effect X_1	3.37	0.41
first effect X_2	2.94	88.71
first effect X_3	83.76	0.68
first effect X_4	0.92	7.81
sum of first effects	90.99	97.61
interaction between X_1 and X_2	0.12	0.01
interaction between X_1 and X_3	0.40	0.00
interaction between X_1 and X_4	0.54	0.00
interaction between X_2 and X_3	0.68	0.00
interaction between X_2 and X_4	1.15	1.26
interaction between X_3 and X_4	2.05	0.00
total effect of X_1	4.43	0.42
total effect of X_2	4.89	89.98
total effect of X_3	86.89	0.68
total effect of X_4	4.66	9.07
sum of total effects	100.87	100.15

In relation with the maximum principal stress, the total effect sensitivity index for the design factor X_2 is 4.89, this value is bigger than the total effect sensitivity index of design factor X_1 which is 4.43, also bigger than the total effect sensitivity index of design factor X_4 which is 4.66, but very much smaller than the total effect sensitivity index of design factor X_3 which is 86.89%, this means that the tensile damage in the tunnel lining is 86.89% due to variation in the Young's modulus of elasticity of the tunnel lining, and it is 4.89% due to the variation in the tunnel diameter, also it is 4.66% due to the variation in the concrete density of the tunnel lining, and it is 4.43% due to the variation in the tunnel lining thickness. It is worthy to mention that the tensile damage in the tunnel lining during seismic action is also related to the interactions between X_2 and X_4 and between X_3 and X_4, which are 1.15 and 2.05, respectively, while the interactions between X_1 and X_2, X_1 and X_3, X_1 and X_4, X_2 and X_3 are not so appreciable
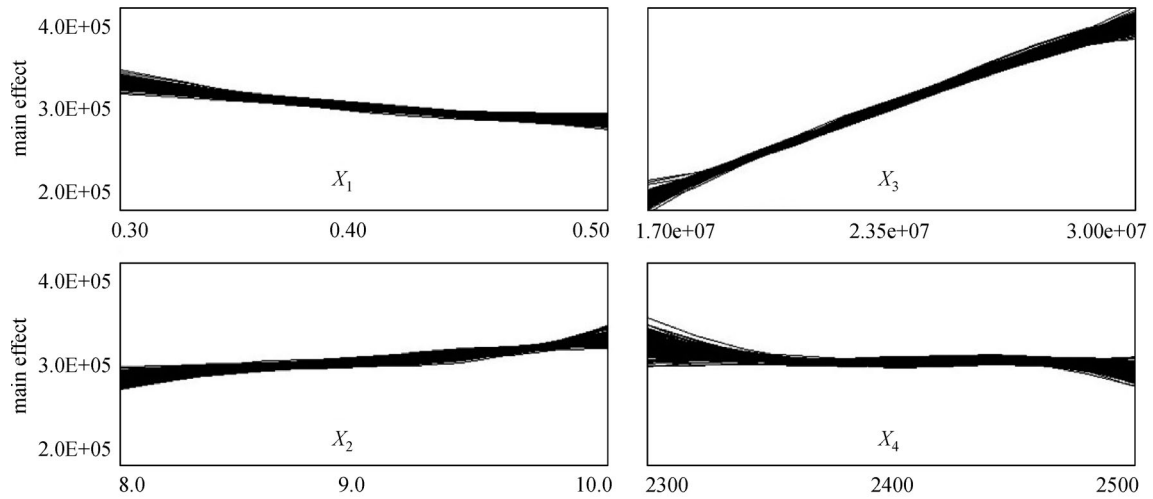
Fig. 3 Main effects of certain factors-maximum principal stress
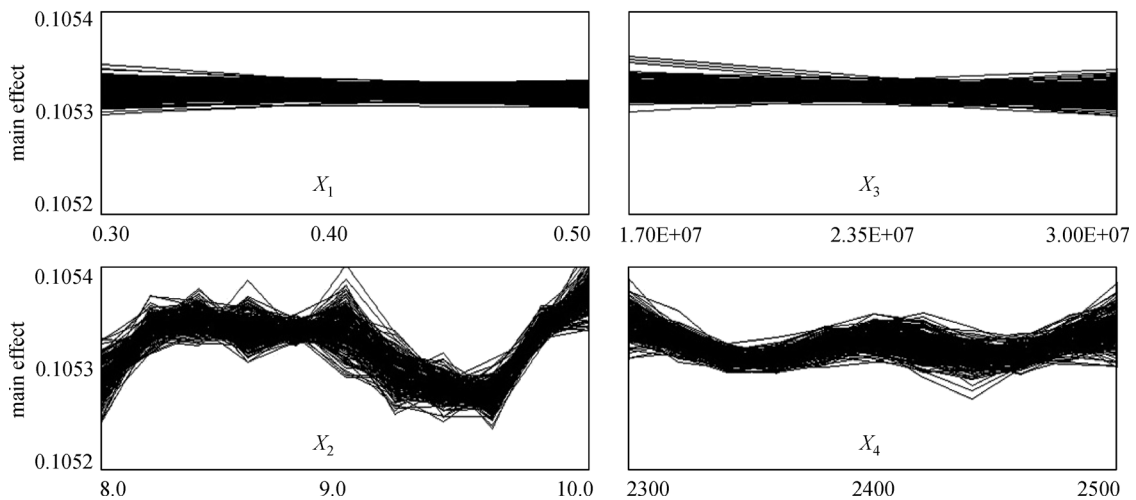

Fig. 4 Main effects of certain factors-maximum overall displacement

compared to the previous two inteactions, which are 0.12, 0.4, 0.54, and 0.68, respectively.

While considering the maximum overall displacement, the total effect sensitivity index for the design factor X_4 is 9.07, this value is bigger than the total effect sensitivity index of design factor X_3 which is 0.68, also bigger than the total effect sensitivity index of design factor X_1 which is 0.42, but very much smaller than the total effect sensitivity index of design factor X_2 which is 89.98%, this means that the stability of the tunnel structure due to seismic action is 89.98% due to variation in the tunnel diameter, and it is 9.07% due to the variation in concrete density of the tunnel lining, also it is 0.68% due to the variation in the Young's modulus of elasticity of the tunnel lining, and it is 0.42% due to the variation in the tunnel lining thickness. Furthermore, we can say that the stability

of the tunnel lining during seismic action is also related to the interactions between X_2 and X_4, which is 1.26, while the interactions between X_1 and X_2, X_1 and X_3, X_1 and X_4, X_2 and X_3, X_3 and X_4 do not exist, which are 0.01, 0.0, 0.0, 0.0, and 0.0, respectively.

5 Results of sensitivity indices—uncertain factors

In the same way, the main effects of the sensitivity indices for each uncertain factor in addition to their interaction effects were calculated targeting the maximum principal stress output of the tunnel lining. Also, the main and interaction effects of sensitivity indices for each uncertain factor were calculated considering the maximum overall

displacement output of the tunnel structure, (see Table 5). Where the main effects of the uncertain factors have been calculated using variation approach, (see Figs. 5 and 6).

Table 5 Sensitivity indices — uncertain factors

sensitivity indices	maximum principal stress	maximum overall displacement
first effect X_5	40.81	99.81
first effect X_6	30.3	0.07
first effect X_7	26.62	0.09
sum of first effects	97.73	99.97
interaction between X_5 and X_6	0.89	0.01
interaction between X_5 and X_7	0.55	0.01
interaction between X_6 and X_7	0.56	0.00
total effect of X_5	42.25	99.83
total effect of X_6	31.75	0.09
total effect of X_7	27.73	0.10
sum of total effects	101.73	100.02

By considering the maximum principal stress, the total effect sensitivity index for the design factor X_5 is 42.25, this value is bigger than the total effect sensitivity index of design factor X_6 which is 31.75, also bigger than the total effect sensitivity index of design factor X_7 which is 27.73. This means that the tensile damage in the tunnel lining is 42.25% due to variation in the peak ground acceleration of the seismic action, and it is 31.75% due to the variation in the soil density, also it is 27.73% due to the variation in the soil modulus of elasticity. Furthermore, the tensile damage in the tunnel lining during seismic action is also related to a small effects of the interactions between X_5 and X_6, X_5

and X_7, X_6 and X_7, which are 0.89, 0.55, and 0.56, respectively.

In the other side related to the maximum overall displacement, the total effect sensitivity index for the design factor X_5 is 99.83, this value is so much bigger than the total effect sensitivity index of design factor X_6 which is 0.09, also so much bigger than the total effect sensitivity index of design factor X_7 which is 0.1. This an indication that the stability of the tunnel structure due to seismic action is 99.83% due to variation in peak ground acceleration, and it is 0.09% due to the variation in soil density which is not appreciable. Also it is 0.1% due to the variation in the soil modulus of elasticity. We can also detect that the stability of the tunnel lining during seismic action is not related to the interactions between X_5 and X_6 which is 0.01, and the interactions between X_5 and X_7, X_6 and X_7 which are 0.01, 0.01, and 0.0, respectively, because of the so low magnitudes of them which approach zero approximately.

6 Results of numerical simulations

Depending on the results of the Sobol's sensitivity indices, the most effective design factors are considered to carry on numerical simulations for the exposure of a circular tunnel to a seismic action with a constant peak ground acceleration of 4.905 m/s² and constant design factors (tunnel thickness, tunnel diameter, tunnel concrete density, soil density and soil modulus of elasticity) regarding tensile damage and the stability of the tunnel.

6.1 Numerical simulations of tensile damage

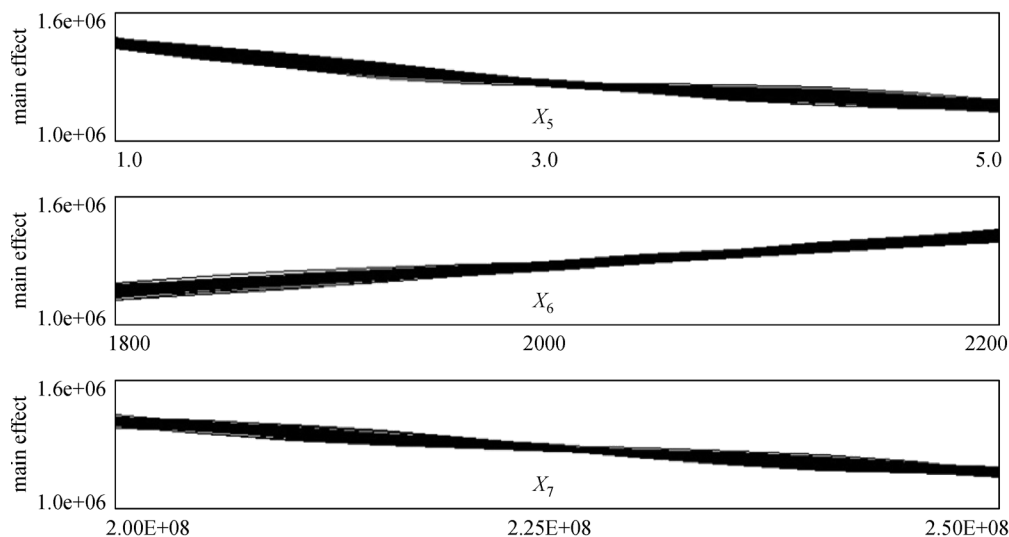For the tensile damage output, the variation in the concrete

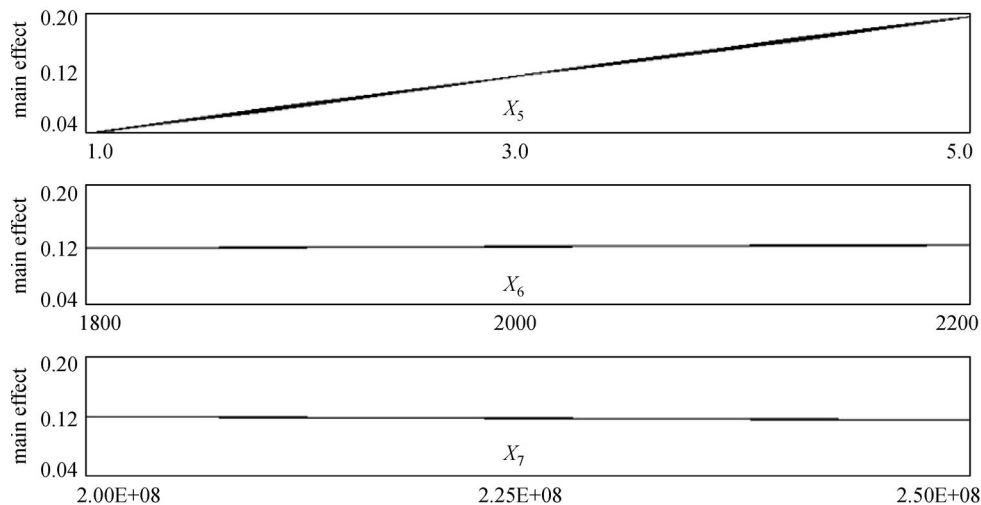**Fig. 5** Main effects of uncertain factors-maximum principal stress

Fig. 6 Main effects of uncertain factors-maximum overall displacement

modulus of elasticity values is dedicated to determine the effects on the tensile damage generation in the tunnel lining where three values are dedicated (23E + 09, 27E + 09, and 31E + 09 Pa).

For minimum value of the concrete modulus of elasticity the maximum principal stress value is 8.366E + 05 Pa, and it is equal to 9.156E + 05 Pa for the medium value of the mentioned factor. While it has a value of 9.383E + 05 Pa for the maximum value. We discover a nonlinear relation between the variation of the concrete modulus of elasticity and the maximum principal stress which is a criteria of the tensile damage in four regions as seen in red color inside the tunnel lining at four regions.The deformations in the tunnel lining increase with the increase of this design factor where a negative maximum principal stress in the surrounding soil shown in light green color in the perpendicular positions to the red regions inside the tunnel lining, see (Figs. 7(a)–7(f)) is an indicator of the increase of the positive maximum principal stress in the tunnel lining. Another indication is the increase of the light green color area with the increase of the value of the mentioned factor.

6.2 Results of stability

While for the stability output, the variation in the tunnel diameter values is dedicated to determine its effects on the stability of the tunnel where three values are considered which are (8.0, 9.0, and 10.0 m) (see Fig. 8).

The variation in the diameter value does not result in an appreciable change in the overal displacement of the tunnel where the change starts obviouslt after eight seconds from the seismic action. It is worthy to mention that the maximum displacements don't reach 0.2 m in all three cases. As a result we discover that in the critical case of diameter design factor the stability of the tunnel won't

change despite the fact that there is a change in the diameter of the tunnel.

7 Conclusions

We can conclude the following aspects supporting on the numerical simulations and the Sobol's sensitivity indices regarding the tensile damage in the tunnel lining and the stability of the tunnel structure during the seismic action:

1) The most effective design factor which is deciding in the generation of tensile damage in the tunnel lining is the concrete modulus of elasticity of the tunnel lining. Also the soil mechanic properties (modulus of elasticity and density) have an appreciable effects on this output results. While the tunnel lining thickness, diameter and conceret density have small effects on the generation of the tensile damage which can be considered safe compared to other mentioned design factors.

2) The interaction between the design factors concrete modulus of elasticity and concrete density has the greatest effect on the generation of tensile damage, also the interaction between the tunnel diameter and the concrete density has the second rank effect on this output. While the interactions between the other design factors have an equal small effects on this output approximately.

3) The most effective design factor which is deciding in the stability of the tunnel structure is the tunnel diameter. Also the concrete density is taking part in the stability process. While the tunnel lining thickness, conceret modulus of elasticity, soil density and soil modulus of elasticty have a very small effects on the stability of the tunnel which can be regarded safe in the design process.

4) The interaction between the design factors tunnel diameter and concrete density has the greatest effect on the
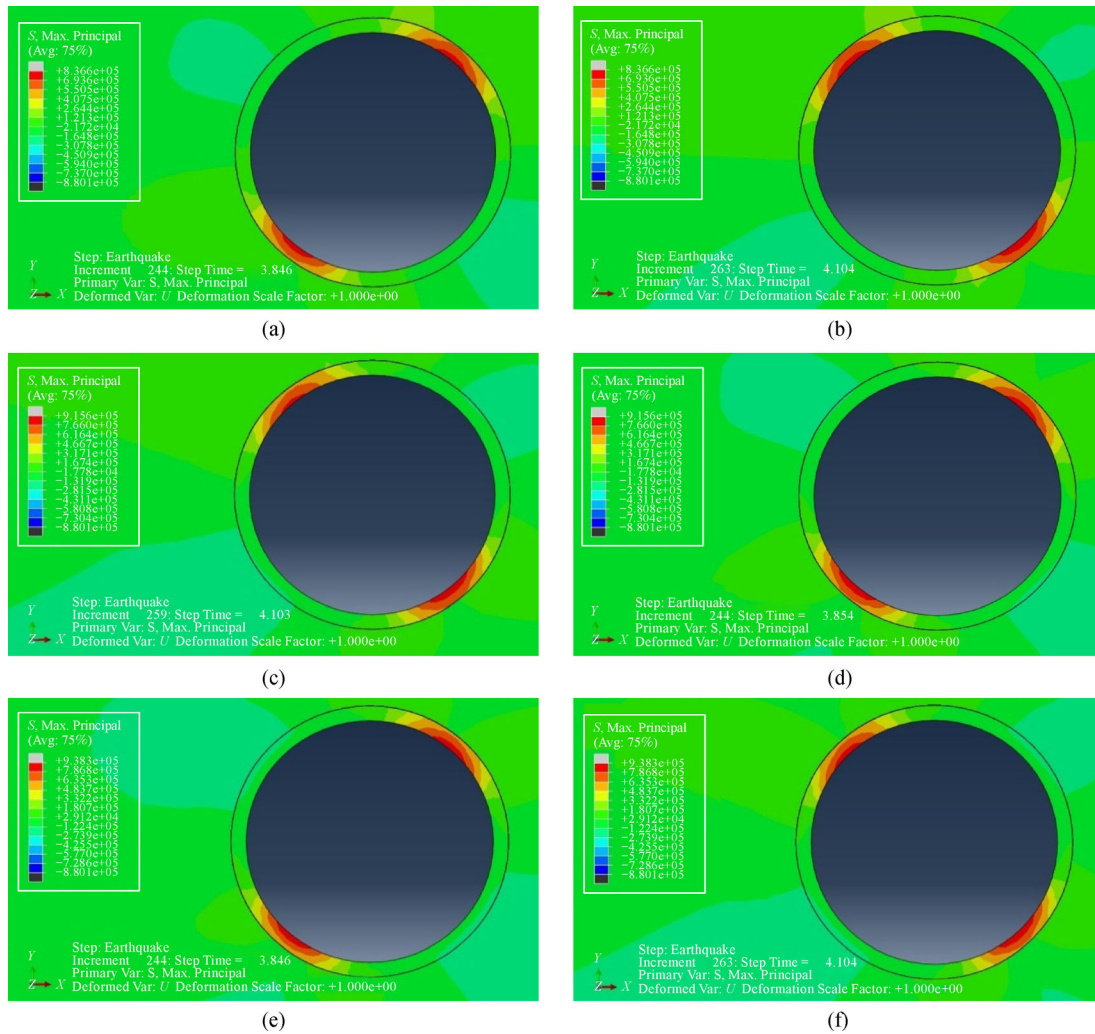
Fig. 7 Variation of concrete modulus of elasticity-tensile damage. (a) Minimum value at time = 3.8 s; (b) minimum value at time = 4.1 s; (c) medium value at time = 3.8 s; (d) medium value at time = 4.1 s; (e) maximum value at time = 3.8 s; (f) maximum value at time = 4.1 s
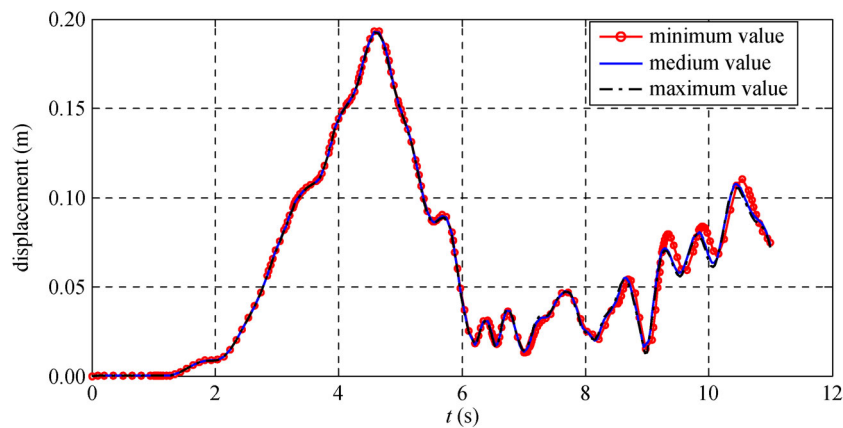

Fig. 8 Variation of tunnel diameter-stability

stability of the tunnel during seismic action which is related to the self weight of the tunnel. Also the interaction between the tunnel thickness and the tunnel diameter has a small appreciable effect on the the stability. While the interactions between the other design factors have zero effects on the stability of the tunnel.

5) The Sobol's sensitivity indices approach manifested a great efficiency in revealing the predicted roles of each certain and uncertain design factors in the generation of tensile damage and stability of the tunnel during seismic actions.

References

1. Akhlaghi T, Nikkar A. Effect of vertically propagating shear waves on seismic behavior of circular tunnels. Hindawi the Scientific World Journal, 2014, 2014, 1–10

2. Hashash Y M A, Hook J J, Schmidt B, I-Chiang Yao J. Seismic design and analysis of underground structure. Tunnelling and Underground Space Technology, 2001, 16(4): 247–293

3. Nariman N A, Hussain R R, Msekh M A, Karampour P. Prediction meta-models for the responses of a circular tunnel during earthquakes. Underground Space, 2019, 4(1): 31–47

4. Nariman N A, Ramazan A, Mohammad I I. Application of coupled XFEM-BCQO in the structural optimization of a circular tunnel lining subjected to a ground motion. Frontiers of Structural and Civil Engineering, 2019 (in press)

5. Mollon G, Dias D, Soubra A H. Probabilistic analysis and design of circular tunnels against face stability. International Journal of Geomechanics, 2009, 9(6): 237–249

6. Kalab Z, Stemon P. Influence of seismic events on shallow geotechnical structures. Acta Montanistica Slovaca, 2017, 22(4): 412–421

7. Ghasemi H, Park H S, Rabczuk T. A level-set based IGA formulation for topology optimization of flexoelectric materials. Computer Methods in Applied Mechanics and Engineering, 2017, 313: 239–258

8. Ghasemi H, Brighenti R, Zhuang X, Muthu J, Rabczuk T. Optimum fiber content and distribution in fiber-reinforced solids using a reliability and NURBS based sequential optimization approach. Structural and Multidisciplinary Optimization, 2015, 51(1): 99–112

9. Zhang C, Nanthakumar S S, Lahmer T, Rabczuk T. Multiple cracks identification for piezoelectric structures. International Journal of Fracture, 2017, 206(2): 151–169

10. Nanthakumar S, Zhuang X, Park H, Rabczuk T. Topology optimization of flexoelectric structures. Journal of the Mechanics and Physics of Solids, 2017, 105: 217–234

11. Nanthakumar S, Lahmer T, Zhuang X, Park H S, Rabczuk T. Topology optimization of piezoelectric nanostructures. Journal of the Mechanics and Physics of Solids, 2016, 94: 316–335

12. Nanthakumar S, Lahmer T, Zhuang X, Zi G, Rabczuk T. Detection of material interfaces using a regularized level set method in piezoelectric structures. Inverse Problems in Science and Engineering, 2016, 24(1): 153–176

13. Nanthakumar S, Valizadeh N, Park H, Rabczuk T. Surface effects on shape and topology optimization of nanostructures. Computational Mechanics, 2015, 56(1): 97–112

14. Nanthakumar S S, Lahmer T, Rabczuk T. Detection of flaws in piezoelectric structures using extended FEM. International Journal for Numerical Methods in Engineering, 2013, 96(6): 373–389

15. Vu-Bac N, Lahmer T, Zhuang X, Nguyen-Thoi T, Rabczuk T. A software framework for probabilistic sensitivity analysis for computationally expensive models. Advances in Engineering Software, 2016, 100: 19–31

16. Vu-Bac N, Silani M, Lahmer T, Zhuang X, Rabczuk T. A unified framework for stochastic predictions of mechanical properties of polymeric nanocomposites. Computational Materials Science, 2015, 96: 520–535

17. Vu-Bac N, Rafiee R, Zhuang X, Lahmer T, Rabczuk T. Uncertainty quantification for multiscale modeling of polymer nanocomposites with correlated parameters. Composites. Part B, Engineering, 2015, 68: 446–464

18. Rabczuk T, Akkermann J, Eibl J. A numerical model for reinforced concrete structures. International Journal of Solids and Structures, 2005, 42(5–6): 1327–1354

19. Bažant Z P. Why continuum damage is nonlocal: Micromechanics arguments. Journal of Engineering Mechanics, 1991, 117(5): 1070–1087

20. Thai T Q, Rabczuk T, Bazilevs Y, Meschke G. A higher-order stress-based gradient-enhanced damage model based on isogeometric analysis. Computer Methods in Applied Mechanics and Engineering, 2016, 304: 584–604

21. Fleck N A, Hutchinson J W. A phenomenological theory for strain gradient effects in plasticity. Journal of the Mechanics and Physics of Solids, 1993, 41(12): 1825–1857

22. Rabczuk T, Eibl J. Simulation of high velocity concrete fragmentation using SPH/MLSPH. International Journal for Numerical Methods in Engineering, 2003, 56(10): 1421–1444

23. Rabczuk T, Eibl J, Stempniewski L. Numerical analysis of high speed concrete fragmentation using a meshfree Lagrangian method. Engineering Fracture Mechanics, 2004, 71(4–6): 547–556

24. Rabczuk T, Xiao S P, Sauer M. Coupling of meshfree methods with nite elements: Basic concepts and test results. Communications in Numerical Methods in Engineering, 2006, 22(10): 1031–1065

25. Rabczuk T, Eibl J. Modelling dynamic failure of concrete with meshfree methods. International Journal of Impact Engineering, 2006, 32(11): 1878–1897

26. Etse G, Willam K. Failure analysis of elastoviscoplastic material models. Journal of Engineering Mechanics, 1999, 125(1): 60–69

27. Miehe C, Hofacker M, Welschinger F. A phase field model for rate-independent crack propagation: Robust algorithmic implementation based on operator splits. Computer Methods in Applied Mechanics and Engineering, 2010, 199(45–48): 2765–2778

28. Amiri F, Millan D, Arroyo M, Silani M, Rabczuk T. Fourth order phase-field model for local max-ent approximants applied to crack propagation. Computer Methods in Applied Mechanics and Engineering, 2016, 312(C): 254–275

29. Areias P, Rabczuk T, Msekh M. Phase-field analysis of finite-strain

plates and shells including element subdivision. Computer Methods in Applied Mechanics and Engineering, 2016, 312(C): 322–350

30. Msekh M A, Silani M, Jamshidian M, Areias P, Zhuang X, Zi G, He P, Rabczuk T. Predictions of J integral and tensile strength of clay/epoxy nanocomposites material using phase-field model. Composites. Part B, Engineering, 2016, 93: 97–114

31. Hamdia K, Msekh M A, Silani M, Vu-Bac N, Zhuang X, Nguyen-Thoi T, Rabczuk T. Uncertainty quantication of the fracture properties of polymeric nanocomposites based on phase-field modeling. Composite Structures, 2015, 133: 1177–1190

32. Msekh M A, Sargado M, Jamshidian M, Areias P, Rabczuk T. ABAQUS implementation of phase-field model for brittle fracture. Computational Materials Science, 2015, 96: 472–484

33. Amiri F, Millán D, Shen Y, Rabczuk T, Arroyo M. Phase-field modeling of fracture in linear thin shells. Theoretical and Applied Fracture Mechanics, 2014, 69: 102–109

34. Hamdia K M, Zhuang X, He P, Rabczuk T. Fracture toughness of polymeric particle nanocomposites: Evaluation of Models performance using Bayesian method. Composites Science and Technology, 2016, 126: 122–129

35. Rabczuk T, Belytschko T, Xiao S P. Stable particle methods based on Lagrangian kernels. Computer Methods in Applied Mechanics and Engineering, 2004, 193(12–14): 1035–1063

36. Rabczuk T, Belytschko T. Adaptivity for structured meshfree particle methods in 2D and 3D. International Journal for Numerical Methods in Engineering, 2005, 63(11): 1559–1582

37. Nguyen V P, Rabczuk T, Bordas S, Duflot M. Meshless methods: A review and computer implementation aspects. Mathematics and Computers in Simulation, 2008, 79(3): 763–813

38. Zhuang X, Cai Y, Augarde C. A meshless sub-region radial point interpolation method for accurate calculation of crack tip elds. Theoretical and Applied Fracture Mechanics, 2014, 69: 118–125

39. Zhuang X, Zhu H, Augarde C. An improved meshless Shepard and least square method possessing the delta property and requiring no singular weight function. Computational Mechanics, 2014, 53(2): 343–357

40. Zhuang X, Augarde C, Mathisen K. Fracture modelling using meshless methods and level sets in 3D: Framework and modelling. International Journal for Numerical Methods in Engineering, 2012, 92(11): 969–998

41. Chen L, Rabczuk T, Bordas S, Liu GR, Zeng KY, Kerfriden P. Extended finite element method with edge-based strain smoothing (Esm-XFEM) for linear elastic crack growth. Computer Methods in Applied Mechanics and Engineering, 2012, 209–212(4): 250–265

42. Belytschko T, Black T. Elastic crack growth in finite elements with minimal remeshing. International Journal for Numerical Methods in Engineering, 1999, 45(5): 601–620

43. Moës N, Dolbow J, Belytschko T. A finite element method for crack growth without remeshing. International Journal for Numerical Methods in Engineering, 1999, 46(1): 131–150

44. Vu-Bac N, Nguyen-Xuan H, Chen L, Lee C K, Zi G, Zhuang X, Liu G R, Rabczuk T. A phantom-node method with edge-based strain smoothing for linear elastic fracture mechanics. Journal of Applied Mathematics, 2013, 2013, 978026

45. Bordas S P A, Natarajan S, Kerfriden P, Augarde C E, Mahapatra D R, Rabczuk T, Pont S D. On the performance of strain smoothing for quadratic and enriched finite element approximations (XFEM/GFEM/PUFEM). International Journal for Numerical Methods in Engineering, 2011, 86(4–5): 637–666

46. Bordas S P A, Rabczuk T, Hung N X, Nguyen V P, Natarajan S, Bog T, Quan D M, Hiep N V. Strain Smoothing in FEM and XFEM. Computers & Structures, 2010, 88(23–24): 1419–1443

47. Rabczuk T, Zi G, Gerstenberger A, Wall W A. A new crack tip element for the phantom node method with arbitrary cohesive cracks. International Journal for Numerical Methods in Engineering, 2008, 75(5): 577–599

48. Chau-Dinh T, Zi G, Lee P S, Rabczuk T, Song J H. Phantom-node method for shell models with arbitrary cracks. Computers & Structures, 2012, 92–93: 242–256

49. Song J H, Areias P M A, Belytschko T. A method for dynamic crack and shear band propagation with phantom nodes. International Journal for Numerical Methods in Engineering, 2006, 67(6): 868–893

50. Areias P M A, Song J H, Belytschko T. Analysis of fracture in thin shells by overlapping paired elements. Computer Methods in Applied Mechanics and Engineering, 2006, 195(41–43): 5343–5360

51. Rabczuk T, Areias P M A. A meshfree thin shell for arbitrary evolving cracks based on an external enrichment. CMES-Computer Modeling in Engineering and Sciences, 2006, 16(2): 115–130

52. Zi G, Rabczuk T, Wall W A. Extended meshfree methods without branch enrichment for cohesive cracks. Computational Mechanics, 2007, 40(2): 367–382

53. Rabczuk T, Bordas S, Zi G. A three-dimensional meshfree method for continuous multiple-crack initiation, propagation and junction in statics and dynamics. Computational Mechanics, 2007, 40(3): 473–495

54. Rabczuk T, Zi G. A meshfree method based on the local partition of unity for cohesive cracks. Computational Mechanics, 2007, 39(6): 743–760

55. Rabczuk T, Areias P M A, Belytschko T. A meshfree thin shell method for nonlinear dynamic fracture. International Journal for Numerical Methods in Engineering, 2007, 72(5): 524–548

56. Bordas S, Rabczuk T, Zi G. Three-dimensional crack initiation, propagation, branching and junction in non-linear materials by an extended meshfree method without asymptotic enrichment. Engineering Fracture Mechanics, 2008, 75(5): 943–960

57. Rabczuk T, Zi G, Bordas S, Nguyen-Xuan H. A geometrically non-linear three dimensional cohesive crack method for reinforced concrete structures. Engineering Fracture Mechanics, 2008, 75(16): 4740–4758

58. Rabczuk T, Gracie R, Song J H, Belytschko T. Immersed particle method for fluid-structure interaction. International Journal for Numerical Methods in Engineering, 2010, 81(1): 48–71

59. Rabczuk T, Bordas S, Zi G. On three-dimensional modelling of crack growth using partition of unity methods. Computers & Structures, 2010, 88(23–24): 1391–1411

60. Amiri F, Anitescu C, Arroyo M, Bordas S, Rabczuk T. XLME interpolants, a seamless bridge between XFEM and enriched

meshless methods. Computational Mechanics, 2014, 53(1): 45–57

61. Talebi H, Samaniego C, Samaniego E, Rabczuk T. On the numerical stability and mass-lumping schemes for explicit enriched meshfree methods. International Journal for Numerical Methods in Engineering, 2012, 89(8): 1009–1027

62. Nguyen-Thanh N, Zhou K, Zhuang X, Areias P, Nguyen-Xuan H, Bazilevs Y, Rabczuk T. Isogeometric analysis of large-deformation thin shells using RHTsplines for multiple-patch coupling. Computer Methods in Applied Mechanics and Engineering, 2017, 316: 1157–1178

63. Nguyen-Thanh N, Valizadeh N, Nguyen M N, Nguyen-Xuan H, Zhuang X, Areias P, Zi G, Bazilevs Y, De Lorenzis L, Rabczuk T. An extended isogeometric thin shell analysis based on Kirchho-Love theory. Computer Methods in Applied Mechanics and Engineering, 2015, 284: 265–291

64. Jia Y, Anitescu C, Ghorashi S, Rabczuk T. Extended isogeometric analysis for material interface problems. IMA Journal of Applied Mathematics, 2015, 80(3): 608–633

65. Ghorashi S, Valizadeh N, Mohammadi S, Rabczuk T. T-spline based XIGA for fracture nalysis of orthotropic media. Computers & Structures, 2015, 147: 138–146

66. Rabczuk T, Belytschko T. Cracking particles: A simplified meshfree method for arbitrary evolving cracks. International Journal for Numerical Methods in Engineering, 2004, 61(13): 2316–2343

67. Rabczuk T, Areias P M A. A new approach for modelling slip lines in geological materials with cohesive models. International Journal for Numerical and Analytical Methods in Engineering, 2006, 30(11): 1159–1172

68. Rabczuk T, Belytschko T. Application of particle methods to static fracture of reinforced concrete structures. International Journal of Fracture, 2006, 137(1–4): 19–49

69. Rabczuk T, Belytschko T. A three dimensional large deformation meshfree method for arbitrary evolving cracks. Computer Methods in Applied Mechanics and Engineering, 2007, 196(29–30): 2777–2799

70. Rabczuk T, Areias P M A, Belytschko T. A simplied meshfree method for shear bands with cohesive surfaces. International Journal for Numerical Methods in Engineering, 2007, 69(5): 993–1021

71. Rabczuk T, Samaniego E. Discontinuous modelling of shear bands using adaptive meshfree methods. Computer Methods in Applied Mechanics and Engineering, 2008, 197(6–8): 641–658

72. Rabczuk T, Song J H, Belytschko T. Simulations of instability in dynamic fracture by the cracking particles method. Engineering Fracture Mechanics, 2009, 76(6): 730–741

73. Rabczuk T, Zi G, Bordas S, Nguyen-Xuan H. A simple and robust three-dimensional cracking-particle method without enrichment. Computer Methods in Applied Mechanics and Engineering, 2010, 199(37–40): 2437–2455

74. Cai Y, Zhuang X, Zhu H. A generalized and ecient method for nite cover generation in the numerical manifold method. International Journal of Computational Methods, 2013, 10(5): 1350028

75. Liu G, Zhuang X, Cui Z. Three-dimensional slope stability analysis using independent cover based numerical manifold and vector method. Engineering Geology, 2017, 225: 83–95

76. Nguyen B H, Zhuang X, Wriggers P, Rabczuk T, Mear M E, Tran H D. Isogeometric symmetric Galerkin boundary element method for three-dimensional elasticity problems. Computer Methods in Applied Mechanics and Engineering, 2017, 323: 132–150

77. Nguyen B H, Tran H D, Anitescu C, Zhuang X, Rabczuk T. An isogeometric symmetric Galerkin boundary element method for two-dimensional crack problems. Computer Methods in Applied Mechanics and Engineering, 2016, 306: 252–275

78. Zhu H, Wu W, Chen J, Ma G, Liu X, Zhuang X. Integration of three dimensional discontinuous deformation analysis (DDA) with binocular photogrammetry for stability analysis of tunnels in blocky rock mass. Tunnelling and Underground Space Technology, 2016, 51: 30–40

79. Wu W, Zhu H, Zhuang X, Ma G, Cai Y. A multi-shell cover algorithm for contact detection in the three dimensional discontinuous deformation analysis. Theoretical and Applied Fracture Mechanics, 2014, 72: 136–149

80. Cai Y, Zhu H, Zhuang X. A continuous/discontinuous deformation analysis (CDDA) method based on deformable blocks for fracture modelling. Frontiers of Structural and Civil Engineering, 2013, 7(4): 369–378

81. Nguyen-Xuan H, Liu G R, Bordas S, Natarajan S, Rabczuk T. An adaptive singular ES-FEM for mechanics problems with singular eld of arbitrary order. Computer Methods in Applied Mechanics and Engineering, 2013, 253: 252–273

82. Areias P, Rabczuk T. Steiner-point free edge cutting of tetrahedral meshes with applications in fracture. Finite Elements in Analysis and Design, 2017, 132: 27–41

83. Areias P, Reinoso J, Camanho P, Rabczuk T. A constitutive-based element-by-element crack propagation algorithm with local mesh refinement. Computational Mechanics, 2015, 56(2): 291–315

84. Areias P M A, Rabczuk T, Camanho P P. Finite strain fracture of 2D problems with injected anisotropic softening elements. Theoretical and Applied Fracture Mechanics, 2014, 72: 50–63

85. Areias P, Rabczuk T, Dias-da-Costa D. Element-wise fracture algorithm based on rotation of edges. Engineering Fracture Mechanics, 2013, 110: 113–137

86. Areias P, Rabczuk T, Camanho P P. Initially rigid cohesive laws and fracture based on edge rotations. Computational Mechanics, 2013, 52(4): 931–947

87. Areias P, Rabczuk T. Finite strain fracture of plates and shells with congurational forces and edge rotation. International Journal for Numerical Methods in Engineering, 2013, 94(12): 1099–1122

88. Silani M, Talebi H, Hamouda A S, Rabczuk T. Nonlocal damage modeling in clay/epoxy nanocomposites using a multiscale approach. Journal of Computational Science, 2016, 15: 18–23

89. Talebi H, Silani M, Rabczuk T. Concurrent multiscale modelling of three dimensional crack and dislocation propagation. Advances in Engineering Software, 2015, 80: 82–92

90. Silani M, Talebi H, Ziaei-Rad S, Hamouda A M S, Zi G, Rabczuk T. A three dimensional extended Arlequin method for dynamic fracture. Computational Materials Science, 2015, 96: 425–431

91. Silani M, Ziaei-Rad S, Talebi H, Rabczuk T. A semi-concurrent multiscale approach for modeling damage in nanocomposites. Theoretical and Applied Fracture Mechanics, 2014, 74: 30–38

92. Talebi H, Silani M, Bordas S, Kerfriden P, Rabczuk T. A

computational library for multiscale modelling of material failure. Computational Mechanics, 2014, 53(5): 1047–1071

93. Talebi H, Silani M, Bordas S P A, Kerfriden P, Rabczuk T. Molecular dynamics/XFEM coupling by a three-dimensional extended bridging domain with applications to dynamic brittle fracture. International Journal for Multiscale Computational Engineering, 2013, 11(6): 527–541

94. Yang S W, Budarapu P R, Mahapatra D R, Bordas S P A, Zi G, Rabczuk T. A meshless adaptive multiscale method for fracture. Computational Materials Science, 2015, 96: 382–395

95. Budarapu P, Gracie R, Bordas S, Rabczuk T. An adaptive multiscale method for quasi-static crack growth. Computational Mechanics, 2014, 53(6): 1129–1148

96. Budarapu P R, Gracie R, Yang S W, Zhuang X, Rabczuk T. Ecient coarse graining in multiscale modeling of fracture. Theoretical and Applied Fracture Mechanics, 2014, 69: 126–143

97. Zhuang X, Wang Q, Zhu H. Multiscale modelling of hydro-mechanical couplings in quasi-brittle materials. International Journal of Fracture, 2017, 204(1): 1–27

98. Zhu H, Wang Q, Zhuang X. A nonlinear semi-concurrent multiscale method for fractures. International Journal of Impact Engineering, 2016, 87: 65–82

99. Zhuang X, Wang Q, Zhu H. A 3D computational homogenization model for porous material and parameters identification. Computational Materials Science, 2015, 96: 536–548

100. Kouznetsova V, Geers M G D, Brekelmans W A M. Multi-scale constitutive modelling of heterogeneous materials with a gradient-enhanced computational homogenization scheme. International Journal for Numerical Methods in Engineering, 2002, 54(8): 1235–1260

101. Rabczuk T, Ren H. A peridynamics formulation for quasi-static fracture and contact in rock. Engineering Geology, 2017, 225: 42–48

102. Amani J, Oterkus E, Areias P, Zi G, Nguyen-Thoi T, Rabczuk T. A non-ordinary state-based peridynamics formulation for thermo-plastic fracture. International Journal of Impact Engineering, 2016, 87: 83–94

103. Ren H, Zhuang X, Rabczuk T. A new Peridynamic formulation with shear deformation for elastic solid. Journal of Micromechanics and Molecular Physics, 2016, 1(2): 1650009

104. Ren H, Zhuang X, Cai Y, Rabczuk T. Dual-horizon peridynamics. International Journal for Numerical Methods in Engineering, 2016, 108(12): 1451–1476

105. Ren H, Zhuang X, Rabczuk T. Dual-horizon peridynamics: A stable solution to varying horizons. Computer Methods in Applied Mechanics and Engineering, 2017, 318: 762–782

106. Glen G, Isaacs K. Estimating sobol sensitivity indices using correlations. Journal of Environmental Modelling and Software, 2012, 37: 157–166

107. Nossent J, Elsen P, Bauwens W. Sobol sensitivity analysis of a complex environmental model. Journal of Environmental Modelling and Software, 2011, 26(12): 1515–1525

108. Zhang X Y, Trame M N, Lesko L J, Schmidt S. Sobol sensitivity analysis: A tool to guide the development and evaluation of systems pharmacology models. CPT: Pharmacometrics & Systems Pharmacology, 2015, 4(2): 69–79